

Quantification of single walled carbon nanotube nucleation for the length amplification of nanotubes

Alvin W. Orbaek^a, Andrew R. Barron^{a,b}.

^aDepartment of Chemistry, Rice University
Houston, TX 77005, United States, aok@ric.edu

^bDepartment of Mechanical Engineering and Materials Science, Rice University
Houston, TX 77005, United States, arb@ric.edu

ABSTRACT

SEM quantification of SWNTs grown per unit area using a Co-Fe (50:50) catalyst system at 900 °C were subjected to secondary growth, using a range of CH₄:H₂ ratios. It was found that nucleation and growth stages are optimal under different conditions. Optimum conditions for nucleation resulted in >10x increase in SWNT density. Optimization is dependent on appropriate temperature conditions coupled with adequate partial pressure of reagent gas species. We intend to apply this approach to develop a catalyst activity map, such that the enrichment of nanotubes with specific chiralities, achieved through length amplification, is not contaminated with newly nucleated nanotubes. Whereby length amplification be employed to create sufficient quantities of SWNTs for large-scale industrial use.

Keywords: carbon nanotube, smart grid, armchair, amplification, nucleation.

1 INTRODUCTION

The growth of single walled carbon nanotubes (SWNTs) from a hydrocarbon source in the presence of a metal nanoparticle catalyst has been extensively studied. The majority of research has been concentrated on iron catalysts, formed from the reduction of preformed iron oxide nanoparticles [1] or the in-situ formation of nanoparticles from iron salts or iron compounds [2]. In an effort to create better catalysts studies have extended to cobalt [3], and nickel [4,5] containing pro-catalysts (precursor to the actual metallic catalyst particle), as well as bi-metallic [2,6] and ternary phase metallic derivatives [7].

For any particular catalyst composition there are four distinct stages that may be considered in the successful growth of a carbon nanotube. First, there is the activation of the pro-catalyst to form a reactive catalyst. This ordinarily involves the chemical (hydrogen) reduction of the oxide pro-catalyst to the metallic state. This reaction provides a particle onto which the hydrocarbon precursor can decompose. The generation of sufficient carbon leads to the second step, which involves the nucleation of a carbon nanotube. At this point, once nucleation occurs, the further

addition of carbon results in SWNT growth, the third step. The final possible phase involves the death of the catalyst (through contamination [8], Ostwald ripening [9], etc). The need to ensure that steps 1 to 3 occur for the maximum number of catalyst particles is nowhere more important than for our concept of SWNT amplification [10]: the process wherein a pro-catalyst particle is attached to a specific chirality SWNT [11,12] then exposed to growth conditions that extend the length (and hence quantity) of that particular SWNT.

We have previously reported the preference for those steps, 1 through 3, as a function of catalyst composition [2]. For example, under identical growth conditions (temperature, pressure, and feedstock composition) cobalt catalysts show a greater propensity for nucleation (i.e. more SWNT per catalyst particles) than the iron analog, but show slower growth rates (i.e. shorter SWNTs). A consideration of this result with literature data shows that comparisons of different catalysts tend to be studied under substantially similar conditions. As such this observation begs the question as to whether it is actually valid to compare different catalysts under the same reaction conditions? After all, the relative efficacy [13] of each catalyst towards activation, through a reduction step, and then SWNT growth, is unlikely to be the same for all metals or catalyst types. Given this issue, is there a simple method to generate an optimum activation map for SWNT growth from metal nanoparticle catalysts?

We have previously shown that the use of metal salt (or metal oxide nanoparticle) doped spin-on-glass thin films provides a suitable substrate and catalyst concentration for the quantitative growth of SWNTs [2]. Furthermore we have reported that under the growth conditions studied only a fraction of the pro-catalyst particles are active but subsequent (secondary) growth occurs if the sample is reintroduced into the growth chamber after analysis. The goal of the present study is to determine the optimum nucleation conditions for a particular catalyst composition as a function of the feedstock composition, i.e., CH₄:H₂ ratio. We propose to use this method to initiate a catalyst 'map' or activation landscape for quantifying SWNT growth.

In our previous work we showed that for Fe-Co catalyst, with a CH₄:H₂ feedstock ratio of 50:50, and a reaction

temperature of 900 °C, nucleation and growth is dependent on the catalyst composition [2]. Under these growth conditions a large number of the catalysts are active for cobalt, such that re-introduction of the SWNT/catalyst sample into the growth chamber does not result in significant number of secondary SWNT growth. At the other end of the composition spectrum (pure iron) only a few of the catalyst are active during each subsequent growth run. Thus, we have chosen Fe-Co catalyst with a 50:50 composition, since this ratio should show sufficient initial growth to provide a baseline, but also have sufficient catalysts that can be activated during secondary growth runs. Thus the system allows for the ready optimization of reaction conditions to determine the percentage of nucleation and growth such that the percentage of active catalysts can be increased.

2 EXPERIMENTAL

Nanoparticles with mean diameter 5 nm were created using 2.5 mM Fe(NO₃)₃, and 2.5 mM Co(NO₃)₂, in a Spin-On Glass solution (Honeywell) on N-type silicon substrates. Multiple samples were exposed to an initial 15 minute growth with CH₄:H₂ of 50:50 (total flow rate = 450 sccm) at 900 °C to provide a baseline for quantifying the number of SWNTs grown from an excess of pro-catalyst. Subsequent secondary growth runs were carried out at a range of CH₄:H₂ ratios from 80:20 to 20:80 to determine the relative amount of new SWNTs that nucleate and grow compared to the baseline value.

3 RESULTS AND DISCUSSION

SWNT quantification per unit area was obtained from SEM images using ImageJ [14]. The substrates were marked at the cardinal points with a scribe to navigate back to specific locations for subsequent imaging. The SEM images in Fig. 1 show a typical example of the results from the first and second growth runs when using CH₄:H₂ 50:50 at 900 °C. As may be seen from Figure 1b the yield after the second growth (new SWNT nucleation) is such that additional catalyst particles were active during the second growth but were dormant in the first growth run. An AFM image of a sample after the first growth (Fig. 2) show that in addition to the SWNTs there are large numbers of nanoparticles forming from the metal salts in-situ within the spin-on-glass substrate. This suggests that the secondary growth is not due to the formation of new nanoparticles (after the initial analysis) during the second growth run. Thus, we propose that the nanoparticles are formed during the initial use of the metal-doped spin-on-glass. In addition, we propose that the new SWNTs formed during the second growth runs, grow from some of these dormant nanoparticle pro-catalysts.

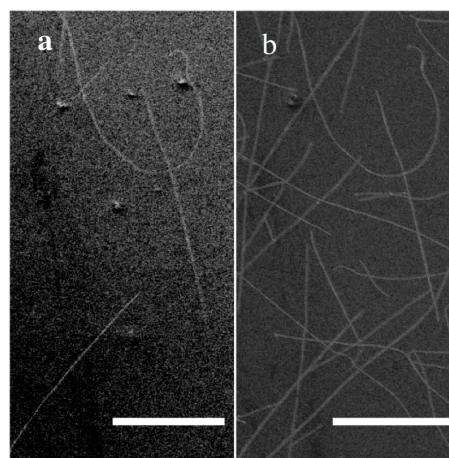


Figure 1: SEM images of SWNT growth showing the results from (a) the first growth and (b) the second growth run. Both were run under the conditions CH₄:H₂ of 50:50 at 900 °C. Scale bar equal to 2.5 μm.

Increasing hydrocarbon feed concentration results in an increased number of catalyst particles growing SWNTs. For example as may be seen from Fig. 3 in comparison to Fig. 1, secondary growth with a CH₄:H₂ ratio of 60:40 shows significantly more new SWNTs (i.e., new nucleation and growth) despite the same number of pro-catalyst nanoparticles. However above 60% CH₄ the SWNT yield decreases. We propose that this is either due to carbon poisoning [15] of the catalyst through the possible formation of a carbon crust, and/or insufficient hydrogen partial pressure to reduce the metal oxide (formed by the exposure of the metal catalyst to the atmosphere during interim analysis), i.e., the pro-catalyst oxide is not converted to the catalyst metal particle.

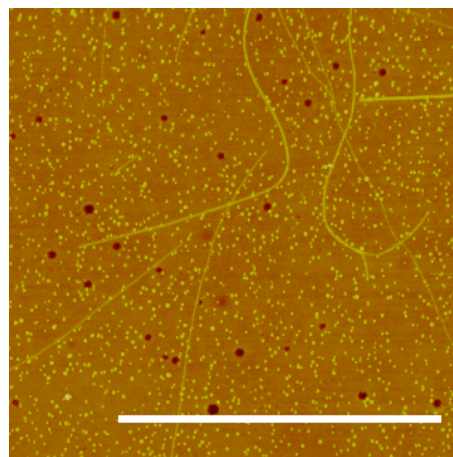


Figure 2: AFM image of SWNT growth using Fe-Co catalyst (50:50) under the conditions of CH₄:H₂ (50:50) at 900 °C. Scale bar equal to 2.5 μm.

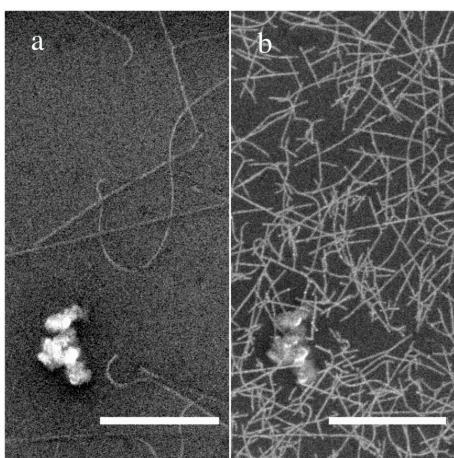


Figure 3: SEM images of SWNT growth showing results from (a) first growth using $\text{CH}_4:\text{H}_2$ of 50:50, and (b) secondary growth from $\text{CH}_4:\text{H}_2$ of 60:40. Scale bar 2.5 μm .

From a comparison of the primary and the secondary growths, the relative nucleation and growth efficiency can be quantified as a function of the feedstock composition ($\text{CH}_4:\text{H}_2$ ratio). The results of this study are shown in Fig. 4. The plot suggests that there is actually a narrow range in which the maximum numbers of pro-catalyst particles are activated, nucleate, and grow SWNTs. It is also interesting to note that the 60:40 $\text{CH}_4:\text{H}_2$ ratio is different from the 50:50 ratios that appear to provide an optimum rate for pure cobalt catalysts [2].

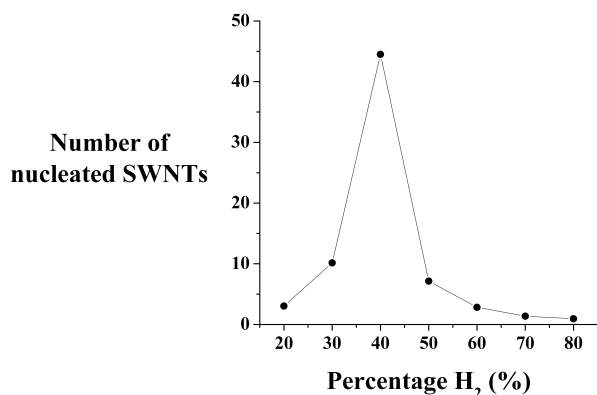


Figure 4: Plot of SWNT yield from the second growth of single walled carbon nanotubes as a function of gas partial pressure of hydrogen.

The implication of this result is that the comparison of different catalyst compositions by growth under identical conditions is not justified or appropriate. This is particularly evident from the difference in SWNT yield of a factor of almost 10 between optimum, and off-set conditions. Instead of a direct comparison we and others have previously employed, we propose it is necessary to ‘map’ the activity (SWNT yield) for each catalyst as a function of feedstock composition. This may also be necessary for other

parameters such as temperature [16], and pressure, and is undoubtedly true for feedstock choice (e.g., CH_4 versus C_2H_2). Only when a suitable activity map is generated can the relative activity of different catalysts be compared. The advantage of the present ‘secondary-growth’ method is that it provides a quantitative comparison between new conditions and standard conditions that can be easily replicated. We are presently undertaking the mapping of a range of catalyst compositions under conditions of growth at 900 $^\circ\text{C}$ with CH_4/H_2 to determine the optimum feedstock ratio for each catalyst composition.

4 CONCLUSIONS

No approach to SWNT growth to date produces only metallic nanotubes with a yield sufficient for industrial use. To remedy this we propose amplifying the lengths of metallic type SWNTs. Within this scenario the nucleation of new SWNTs, invariably of a random chirality, is detrimental to our end goal of producing a large-scale wire of metal only nanotubes. As such it is of practical importance to understand the dynamics of SWNT nucleation, such that it can be avoided when attempting to amplify a batch of chirality specific SWNTs. To this end we propose our method to determine a catalyst activity map to serve as a practical approach for optimizing a high throughput of exclusively amplified, and hence, metallic nanotubes. In this work we find that for the Fe-Co (50:50) system, nucleation is best achieved at a $\text{CH}_4:\text{H}_2$ ratio of 60:40, as evidenced by >10 increase in the number of SWNTs. If this catalyst composition is to be used for large-scale amplification then these conditions, that favor nucleation, must be avoided to prevent contamination of amplified samples with new SWNTs of varying chirality.

REFERENCES

- [1] N. T. Alvarez, A. Orbaek, A. R. Barron, J. M. Tour, and R. H. Hauge, *ACS Appl. Mater. Interfaces*, 2, 15, 2010.
- [2] C. A. Crouse, B. Maruyama, R. Colorado, Jr. T. Back, and A. R. Barron, *J. Am. Chem. Soc.*, 130, 7946, 2008.
- [3] Z. Hongwei, S. Kazutomo, W. Jinqun, W. Kunlin, and W. Dehai, *J. Crys. Growth*, 310, 5473, 2008.
- [4] M. Paillet, V. Jourdain, P. Poncharal, J. L. Sauvajol, A. Zahab, J. C. Meyer, S. Roth, N. Cordente, C. Amiens, and B. Chaudret, *J. Phys. Chem. B*, 108, 17112, 2004.
- [5] S. Reich, L. Li, and J. Robertson, *Chem. Phys. Lett.*, 421, 469, 2006.
- [6] R. E. Anderson, R. Colorado, Jr., C. Crouse, D. Ogrin, B. Maruyama, M. J. Pender, C. L. Edwards, E. Whitsitt, V. C. Moore, D. Koveal, C. Lupu, M. Stewart, J. M. Tour, R. E. Smalley, and A. R. Barron, *Dalton Trans.*, 3097, 2006
- [7] Y. Tian, H. Yang, Y. Cui, S. Zhan, and Y. Chen, *Chem. Commun.*, 2008, 3299.

- [8] G. Zhang, D. Mann, L. Zhang, A. Javey, Y. Li, E. Yenilmez, Q. Wang, J. McVittie, Y. Nishi, J. Gibbons, and H. Dai, *P Natl Acad Sci*, 102, 16141, 2005.
- [9] P. B. Amama, C. L. Pint, L. McJilton, S. M. Kim, E. A. Stach, P. T. Murray, R. H. Hauge, and B. Maruyama, *Nano Lett.*, 9, 44, 2009.
- [10] R. E. Smalley, Y. Li, V. C. Moore, B. K. Price, R. Colorado, H. K. Schmidt, R. H. Hauge, A. R. Barron, and J. M. Tour, *J. Am. Chem. Soc.*, 128, 15824, 2006.
- [11] S. Ghosh, S. M. Bachilo, and R. B. Weisman, *Nature Nanotech.*, 5, 443, 2010.
- [12] E. H. Haroz, W. D. Rice, B. Y. Lu, S. Ghosh, R. H. Hauge, R. B. Weisman, S. K. Doorn, and J. Kono, *J. ACS Nano*, 4, 1955, 2010.
- [13] G. L. Hornyak, L. Grigorian, A. C. Dillon, P. A. Parilla, K. M. Jones, and M. J. Heben, *J. Phys. Chem. B*, 106, 2821, 2002.
- [14] M. D. Abramoff, P. J. Magelhaes, and S. J. Ram, *Biophotonics International*, 11, 36, 2004.
- [15] M. Picher, E. Anglaret, and V. Jourdain, *Diamond & Related Materials*, 19, 581, 2010.
- [16] A. W. Orbaek, A. Owens, A. R. Barron, *Nano Lett.*, 11, 2871, 2011.